Controlling Crystallization: A Key Factor during 3D Printing with the Advanced Semicrystalline Polymeric Materials PEEK, PEKK 6002, and PEKK 7002

Macromolecular Materials and Engineering
Open Access
www.mame-journal.de

Controlling Crystallization: A Key Factor during 3D Printing with the Advanced Semicrystalline Polymeric Materials PEEK, PEKK 6002, and PEKK 7002

Krzysztof Rodzeń, Alistair McIlhagger, Beata Strachota, Adam Strachota, Brian J. Meenan, and Adrian Boyd**

Controlling the crystallization of advanced, high-performance polymeric materials during 3D printing is critical to ensure that the resulting structures have appropriate mechanical properties. In this work, two grades of polyetherketoneketone (PEKK 6002 and PEKK 7002) are used to print 3D specimens via a fused filament fabrication process. The samples are compared with polyetheretherketone printed under the same conditions. Two approaches for controlling the crystallization process are undertaken. The first involves adjustment of the chamber temperature between room temperature and 190 °C to create two regions where crystallization is governed by the slow diffusion process and elevated by limiting the nucleation process. The second approach involves selection of PEKK materials with varying crystallization kinetics, namely. Application of this method into 3D-printing process allows for printing semicrystalline materials with tailored mechanical, thermal, and chemical properties as either amorphous or in situ crystallized products. The studies undertaken here provide the basis to eliminate expensive and time-consuming post-processing of 3D fabricated parts. In particular, solutions for the avoidance of poor adhesion to the building plate and weak interlayer adhesion that can lead to warping are described. The materials are divided into three groups, slow, moderate, and too fast crystallization kinetics.

1. Introduction

Polyaryletherketones (PAEKs) are a class of high-performance semicrystalline thermoplastic materials.[1] Their remarkable mechanical, thermal, and chemical resistance properties are due to the highly aromatic character of the polymeric backbone leading to increased stiffness and crystallization of the products they are used to fabricate.[2] PAEK materials can be processed in the same way as ordinary thermoplastic materials, including via injection molding, extrusion, powder coating, compression molding, computer numerical control machining, or additive manufacturing (AM) to create a range of useful products.[3–5] Many industrial sectors are now using the PAEK family of thermoplastics either in their pristine form or as a composite with other materials for advanced engineering applications in areas such as aerospace, automotive, oil and gas, electronic devices, semiconductors, food processing, and medical due to their favorable properties and significant advantages that they provide in comparison to other polymeric materials and metals.[6–9]

Two AM techniques are commonly used to process PAEK materials, selective laser sintering (SLS) and fused filament fabrication (FFF).[10,11] Commercially available materials and composites mostly used in 3D printing (3DP) are polyetherketonketone (PEKK) and polyetheretherketone (PEEK). Pure materials and composites with up to 20 wt% are mostly used in FFF. Higher content of the filler leads to increased viscosity, which is problematic during filament extrusion.[12] This increases its brittleness and presents difficulty for their storage and handling. In their natural state, PEKK and PEEK do not absorb laser light well which leads to them being brittle post 3DP. For this reason, these materials are often mixed with dark fillers, such as carbon black or carbon fiber to increase the absorption of the laser in SLS 3DP and improve their mechanical properties. The powder used during the 3DP process cannot be reused, which alongside the technique not being open-sourced, means SLS printing of PAEK polymers can be expensive. An additional limitation in SLS printing is the incorporation of brighter fillers, such as hydroxyapatite (HAp), due to their reflective characteristics, which results in mixed precomposite's tensile strength being reduced from 38 MPa (for the pure matrix) to 19 MPa (with 15 wt% HAp filler).[13] Furthermore, PEKK, with an absorption coefficient (*K*)

K. Rodzeń, A. McIlhagger, B. J. Meenan, A. Boyd
School of Engineering
Ulster University
Newtownabbey, Co. Antrim, Northern Ireland BT37 0QB, UK
E-mail: kp.rodzen@ulster.ac.uk; ar.boyd@ulster.ac.uk
B. Strachota, A. Strachota
Institute of Macromolecular Chemistry v.v.i.
Academy of Sciences of the Czech Republic
Heyrovskeho nam. 2, Praha CZ-162 00, Czech Republic
The ORCID identification number(s) for the author(s) of this article can be found under https://doi.org/10.1002/mame.202200668

DOI: 10.1002/mame.202200668

of 0.4 reflects up to 60% of laser light.[14] By comparison, FFF 3DP of PEEK/HAp composites with between 0 and 30 wt% has a tensile strength of 79.5–94.2 MPa.[15] The open-source character of the FFF printers allows for their modification according to their needs of the materials and pushes forward the limits and scope of potential commercial solutions.

The key parameter that determines the printability of advanced semicrystalline polymers is the crystallization time. An ideal situation is when deposition occurs onto an amorphous material to create a new layer on top of one already deposited by FFF. This allows for strong interaction between the layers and reduces anisotropy of the body in the *Z*-direction thus providing acceptable interlayer connection. However, deposition onto an already fully crystallized polymer leads to a reduction in the mechanical properties due to weak bonding. Crystals form a thermal shield for a newly printed layer which has a significantly lower tendency to melt in comparison with an amorphous material. This can lead to defects and strong anisotropy with a 3DP body created with advanced semicrystalline materials and weak mechanical properties in the *Z*-direction. For advanced semicrystalline materials such as PEEK or PEKK, their homopolymer crystallizes rapidly and their crystallization half-time is around 1 s depending on the molecular weight of the polymer chains.[16,17] The crystallization half-time increases with the length of the backbone chain but does not change it significantly.[18]

PEEK is obtained via the reaction of 4,4'-difluorobenzophenone with the disodium salt of hydroquinone with the conditions employed during reaction then resulting in polymer chains with different lengths.[19] Thus, it is possible to get low, medium, and high viscous grades of PEEK with the latter having the longest chain. Low viscous materials are perfect for compounding with fillers but 3DP with virgin low viscous PEEK material is difficult due to the strong tendency to stringing; the filler helps to reduce this problem by increasing melted polymer viscosity.

An interesting alternative that could positively influence the crystallization rate would be partially replace 4,4'-difluorobenzophenone with 3,5′-difluorobenzophenone thereby introducing irregularity into the rigid polymer chain, thus longer crystallization times could be achieved.[20] As it was made by Vitrex for AM 200 to obtain materials with slow crystallization kinetics.[21]

This was achieved for the PEKK family of the materials. The homopolymer of PEKK is synthesized from diphenyl ether and terephthalic acid. In such a form, its crystallinity rate is similar to PEEK. However, partial replacement of the terephthalic acid by isophthalic acid leads to an associated replacement of the para phenyl links with meta phenyl links. Incorporation of the isophthalic acid with its meta phenyl links then increases the crystallization half-time by decreasing the chain regularity, so that a crystalline phase cannot be formed so easily at a large scale.[22] This change positively affects the 3D printability of the PEKK materials and achieves almost isotropic mechanical properties in all directions, which is highly desirable.

The selection of the materials for additive manufacturing is very often based on properties achieved for specimens that have been produced by an injection molding process, with the expectation of similar performance of the materials in the 3DP process. For this reason, PEEK is often selected as a material for 3DP due to its mechanical properties and processing temperature as shown in **Table 1**.[23] This approach is not ideal, especially in the case of other advanced semicrystalline polymers in the PAEK family due to it different crystallization kinetics.

Table 1. Selected properties of the PAEK family based on datasheet injection molded specimens and printing parameters used during sample preparation.

Properties Materials	Tensile modulus [MPa]	T_g [°C]	T_m [°C]
PEKK 6002	2900	160	305
PEKK 7002	3800	162	332
PEEK 450G	4200	143	343

Printing parameters	Value
Nozzle diameter	1 mm
Layer thickness	0.1 mm
Nozzle temperature	360 °C
Building plate	180 °C
Printing speed	40 mm s^{-1}
Raster angle	90°
Current with two 500 W IR lamps	0–3.0 A

The work reported here is a part of a wider investigation into advanced semicrystalline polymeric materials from the PAEK family printed on a modified Ultimaker 2+ (UM2+), which can set a chamber temperature up to 230 °C, print-bed temperature up to 340 °C, and a nozzle temperature of up to 420 °C. The properties of test specimens made from both PEKK 6002 and PEKK 7002 at different chamber temperatures have been investigated and the results were compared with published findings for similar systems created for PEEK, along with the PEEK/HAp and CF/PEEK composite systems. The data obtained here can be used as a vital guide for the selection of the appropriate material for composite preparation after considering the target utilization of printed parts. The article sheds new light on the complex 3DP of advanced semicrystalline materials and their composites using FFF. These studies have three main goals: to determine the most effective strategy for controlling the crystallization process during deposition of layers, to determine the best material for additive manufacturing processes, and to classify polymers according to their crystallization kinetics and the results obtained after the AM process. The additional goal was to optimize the 3DP process for this polymer. Current studies of crystallization kinetics for PEEK 151 and AM 200 suggested a division of polymers into two regions with slow and fast crystallization kinetics.[21] Our findings complement these studies and propose a division into three groups with too-slow, moderate, and too-fast crystallization kinetics, clearly suggesting which group should be selected for the FFF process.

2. Experimental Section

2.1. Materials

PEKK 6002 powder (Hebei Bonster Technology Co., Ltd.) with medium viscosity index (MVI) 6 cc/10 min to 380 °C/1 kg,

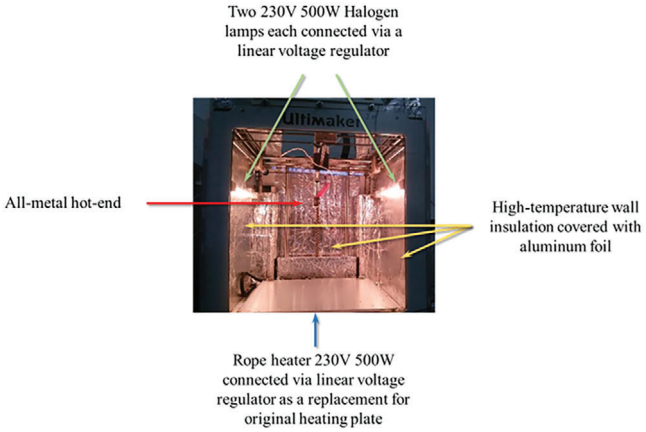

Figure 1. Modifications applied to the UM2+ to print advanced materials and their composites.

viscosity 550 Pa s 1 Hz/380 °C, number average molecular weight M_n = 70 kg mol^{-1} and weight average molecular weight M_w = 30 kg mol^{-1} was processed by a co-rotating twin-screw extruder (Rheomex PTW16/40 OS) with $L/D = 40$ and a diameter of 16 mm was utilized to compound the PEKK into filaments with a diameter of 1.75 mm (±0.10 mm). PEKK 6002 was extruded with screw speed of 45 rpm and an exact melt temperature of 340 °C which was measured in the die. The screw elements were constituted of feed screw elements for the forward and reverse conveying of materials in the feeding, conveying, reverse, venting, and extrusion parts of the extruder and mixing elements of 90° and 0° for providing 30°, 60°, and 90° twist angles for the melting and mixing parts of the extruder. Before extrusion, the powders were dried for 24 h at 150 °C in an oven with air circulation.

PEKK 7002 filament PEKK-SC (Kimya, France) was characterized by the same MVI, viscosity, M_n, M_w as PEKK 6002 and was dried at 120 °C in drying oven for 24 h prior 3DP process filament.

PEEK, PEEK/HAp, CF/PEEK material was the reference from the previous study and was extruded with the same screw setup.[15,24]

2.2. 3DP Process

Printing parameters were the same for both the studied matrixes (PEKK 6002 and 7002) and are placed in Table 1, PEEK and PEEK/HAp materials were printed in the same setup in previous work.[15]

To be able to print advanced materials and composites with a commercial low-temperature printer, it was necessary to raise the temperature of the nozzle and bed and to be able to control the temperature during the deposition process. The modification consisted in installing halogen lamps with the possibility of voltage regulation through a linear voltage regulator. The original bed heater was replaced with a 230 V 500 W line heater with a linear voltage regulator. The hot end was replaced with an all-metal E3D hot end volcano series. Finally, the printer's walls were insulated and covered with aluminum foil to reflect the heat generated by the lamps to the printer's center, **Figure 1**.

The current at two parallel connected 500 W halogen lamps was changed between 0.0 and 3.0 A to adjust the chamber temperature. The 3DP process was followed by a thermal camera and images were taken after homing the building plate. The wall with dimensions of 120 × 70 × 3 mm was printed to eliminate the nozzle's effect, which also participated in heating the 3D printed part. It was expected that obtained data could be applied to large objects.

2.3. Methods

X-ray diffraction (XRD) measurements were performed using an Empyrean diffractometer (Malvern Panalytical, Netherlands) operating at 45 kV and 40 mA using a Cu $K\alpha$ radiation ($\lambda = 1.54187$ Å). Diffractograms were measured over the range of 2-Theta (θ) from 3° to 70° with an angular step interval of 0.0394°. XRD plot was also used to calculate crystallinity as Crystallinity(%) = [(Area of the crystalline peaks)/(Total area of peaks)] × 100 and crystal grain size from the Scherrer equation $\tau = (K \bullet \lambda)/(\beta \bullet \cos\theta)$, where τ is the mean size of the crystalline domains, K is the shape factor equals 1, λ is the X-ray wavelength, β is the full-width at half-maximum, and cosθ is the Bragg angle.

Scanning electron microscopy analysis was performed using a Hitachi SU5000 field emission instrument equipped with an X-MaxN 80 mm^2 silicon drift detector (Oxford Instruments, UK). An acceleration voltage of 10 KeV was used during imaging. Samples were coated with a thin layer (20 nm) of Au/Pd (60/40 ratio) to make the surface of the samples conductive for electron microscopy. The coating was performed using an Emitech K500X sputtering deposition system with argon gas plasma.

Dynamic thermomechanical analysis (DMTA) of the printed specimens was performed with rectangular platelet after water-jet cutting, sized 50 × 10 × 3 mm (about 0.12 in), using an ARES G2 apparatus (TA Instruments, USA). An oscillatory shear deformation (0.1%) at the constant frequency of 1 Hz and at the heating rate of 1–20 °C min^{-1} was applied, and the temperature dependences of the storage shear modulus and of the loss factor (G' and tan(δ), respectively) were recorded. The temperature range was typically from 50 to 380 °C.

Thermal imaging was performed using a Thermal camera GTC 400 C (Bosch, Germany) with the ability to detect temperatures in the range of −10 and +400 °C. Analysis of the pictures was done in dedicated GTC Transfer Software.

3. Results and Discussion

3.1. Influence of Thermal Environment and Type of Material on Thermomechanical Properties, Morphology in Relation to Crystallization Kinetics

The temperatures measured in the middle of the specimen were almost the same up to 2 A for both matrixes as far as crystalline fraction was not generated (**Figure 2**). At 2.5 A, it is possible to notice a generation of the crystalline domains as introducing characteristic opaque beige regions for PEKK 7002. Followed by differences in detected temperature of 132 °C for 6002 and 144 °C for 7002. Printing at 3.0 A caused increasing differences between

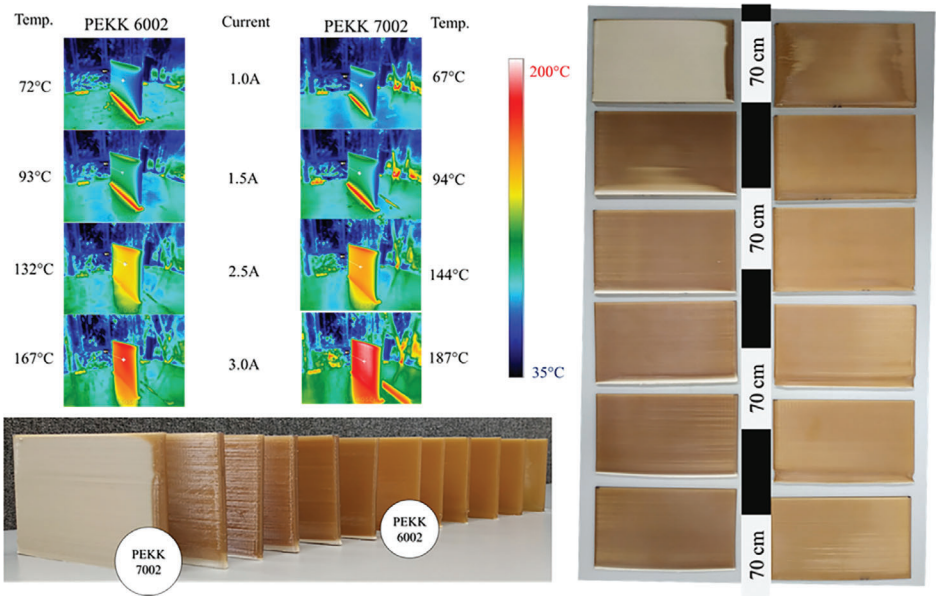

Figure 2. Selected thermal images captured when 3DP was completed and platformed back to the home position for PEKK 6002 and 7002, left-hand side. Current on the lamp was set at 0.0, 1.0, 1.5, 2.0, 2.5, and 3.0 A. Pictures of 3D-printed specimens 120 × 70 × 3 mm, right-hand side.

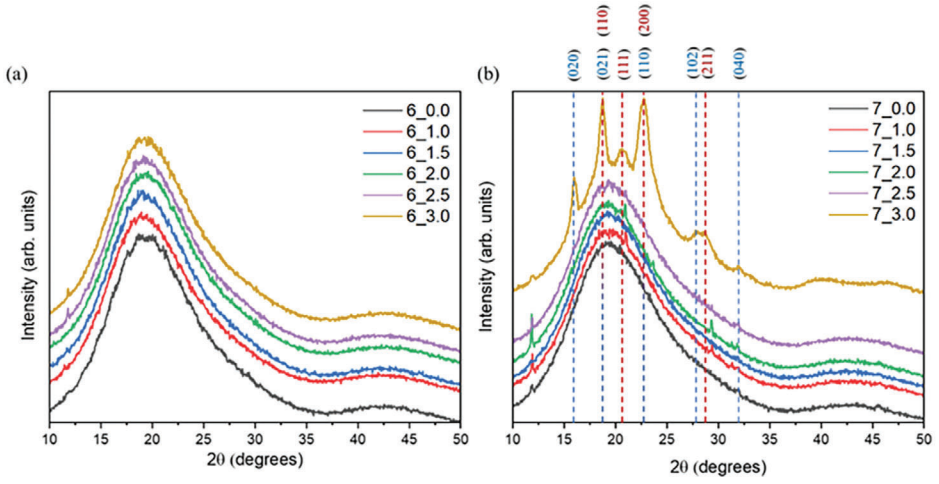

Figure 3. XRD patterns of samples printed with current 0–3 A at two 500 W IR heating lamps for a) PEKK 6002 and b) 7002.

both matrices and for 6002, temperature was 167 °C whereas for 7002 it was 187 °C. Such high chamber temperature for the PEKK 7002, characterized by faster crystallization kinetics allowed to obtain 3DP specimens rich in crystalline phase without additional time-consuming and cost-effective post-curing annealing (Figure 2).

The same conditions were used in our previous investigation of CF/PEEK materials and the recorded temperature in the center of a sample with the same shape was 230 °C at 3.0 A.[24] The difference in the temperature is significant. In the case of CF/PEEK, the black color of the material filled with carbon fiber increases the light absorption, so that more energy is stored in the samples. Amorphous PEKK 6002 and 7002 are slightly brown and partially translucent to light, so a portion of the energy passes through the materials and is lost. When 7002 turns to crystalline, the light cannot pass through the beige, opaque material anymore more and energy is absorbed, but also some has been reflected due to the bright nature of the specimens. Thus, the temperature at 3.0 A recorder for black CF/PEEK was the highest, for light-reflecting beige, opaque 7002 it was lower, and finally for amorphous translucent 6002 was lowest.

3.1.1. Crystallinity as Observed by XRD Spectroscopy

XRD analysis showed the amorphous nature of the samples printed in 3D, especially PEKK 6002 due to the slow crystallization kinetics, crystals are not formed, and only amorphous halo is visible for all samples (**Figure 3**a). A comparable situation can be observed for PEKK 7002 matrix printed where only the highest temperature 187 °C causes a partially crystalline character of the semicrystalline materials with characteristic reflection

peaks (Figure 3b). The total amount of the crystalline fraction was 23.4% with a grain size of 14.66 nm. The PEEK printed with the same lamp current reached the level of 44.6% with a crystallite size of 15.58 nm.[2] In case of PEEK, due to a lower glass transition temperature of about 154 °C and much faster crystallization kinetics above 175 °C, the PEEK crystallization is immediate, and the matrix can reach 95% relative crystallinity within seconds.[25] In contrast to quickly crystallizing PEEK, PEKK 6002 reaches around 1% of relative crystallinity after 60 min while PEKK 7002 gets 1% in 10 min at temperatures around 187 °C.[26] When PEEK was printed (deposited), transparent lightly amber material turned into the opaque beige one instantly just after deposition, while the same layer still was being printed.[15] With PEKK 7002 printed at the same temperature, it was necessary to print a few layers to observe changes in the color of the printed part, which was direct evidence of emerging crystalline structure. Finally for 6002 that change in the color was not observed at all.

PEKK during its crystallization can create two forms of the crystal unit, depending on conditions. The form 1 "two-chain orthorhombic" with planes position (110) ($2\theta = 18.69°$), (111) ($2\theta = 20.61°$), (200) ($2\theta = 22.82°$), and (211) ($2\theta = 28.59°$), respectively, is promoted when melt crystallization occurs (Figure 3b, red numbers). The form 2 "one-chain orthorhombic" is promoted during cold crystallization with planes position (020) ($2\theta = 15.97°$), (021) ($2\theta = 18.73°$), (110) ($2\theta = 22.71°$) and (102) ($2\theta = 27.83$), (120) and (040) ($2\theta = 32.08°$) (Figure 3b, blue numbers).[27,28] Form 1 is thermodynamically more stable and can be formed when the movement of the chain is not restricted. The crystals of form 1 possess a higher melting point and this phase often is called primary. Form 2 is formed when chain mobility is restricted and emerges during the cold crystallization process. It is a less thermodynamically stable phase, melts at lower temperature, and its crystals are called secondary crystals. Secondary crystals melting temperature relates to the temperature used during cold crystallization: this phase is obtained very often as an additional crystalline fraction during the annealing process of 3D printed parts between glass transition temperature and melting point.[29]

PEKK 7002 XRD pattern showed the presence of two types of crystal units for specimen printed at 3 A, Figure 3b. The primary crystals were formed during slow gradual cooling down, where mobility of the chain was the highest till the sample cooled down to a temperature of 190 °C. The secondary crystals were formed during in situ annealing, when the specimen was kept for a longer time at that temperature (190 °C) during the 3DP process. However, at 190 °C chain mobility was already restricted and thus the secondary crystalline phase was formed, not the primary. The primary crystalline phase is responsible for thermal resistance, while secondary crystals which can melt at lower temperatures reduce not only the thermal operating window of the 3D printed part, but also its chemical resistance and mechanical properties. Thus, annealing after the 3DP process is not extremely helpful, because the generation of additional crystallites of the primary phase would be the desired process. To generate primary crystals by cold crystallization, the temperature must be close to the melting point of the polymer (literature example: PEKK: 340 °C), to eliminate the presence of the second fraction.[26] Post-curing at such an elevated temperature can lead to warping and deformation of the printed part. Based on the XRD data (Figure 3b), especially in view of the high intensity of the peak related to plane (111), the dominant crystal unit for the 7_3.0 specimen (PEKK 7002, lamp current: 3.0 A) is the thermodynamically more stable primary phase. Peaks intensity was between PEKK isothermally crystallized at 310 and at 340 °C, where chain relaxations are not limited.[27] This demonstrates the advantages of printing at elevated chamber temperatures if a product with a high crystalline content is desired.

3.1.2. Heating Rate versus Crystallization Kinetics: Evaluation via Mechanical Properties (DMTA)

DMTA analyses with different heating rates were performed to determine the ability for crystallization of both the studied matrixes (PEKK 6002 and 7002) which significantly differ in their crystallization kinetics (see **Figure 4**). The thermo-mechanical tests visualize the cold crystallization processes: these are the "upward steps" in the curves of the storage modulus, which occurred at temperatures above the glass transition (which in turn is visible as a "downward step" in the curves, above 150 °C). After the cold crystallization, a second "downward step" follows, which corresponds to the melting of crystallites.

As the heating rate increased, the cold crystallization shifted strongly toward higher temperatures. Additionally, the "crystallization steps" diminished in size with the heating rate, especially for PEKK 6002, while this behavior is less noticeable for PEKK 7002.

Cold crystallization is a dynamic process which occurs above the temperature of glass transition and below the melting point, and crystals can form only when there is enough time to initiate the crystallization by nucleation, and when the subsequent growth of crystalline domains is continuous.[30] If the heating rate in the DMTA experiments in Figure 4 is too fast compared with too slow crystallization kinetics, the amorphous phase which was initially present in the cold solid polymer will turn into a viscous melt without any cold crystallization step. This kinetics effect is visible if comparing PEKK 6002 characterized by slow crystallization with PEKK 7002 which has a more regular molecular arrangement and thus displays faster crystallization. For PEKK 6002, the rate 10 °C min^{-1} caused a strong reduction of the step related to cold crystallization of the amorphous region (Figure 4a)—blue line, whereas for PEKK 7002 with the same rate it is still possible to observe a distinct cold crystallization step (Figure 4b)—blue line.

DMTA profile analysis shows also that crystals are not formed instantly after crossing the T_g and it is necessary to reach the temperatures where polymer chains can move freely and rearrange into crystalline domains. For PEKK 6002, it would be around at least 210 °C and for PEKK 7002, 180 °C. Below those temperatures is the region where the crystallization process is limited by the slow migration ("diffusion") of polymer chain segments.

3.1.3. Effect of Printing Chamber Temperature on Thermo-Mechanical Properties (DMTA)

Figure 5a shows that the storage modulus at 100 °C (glassy state) for PEKK 6002 printed with a range of chamber temperatures (samples: 6_0.0–6_3.0) was always around 715 MPa (±15).

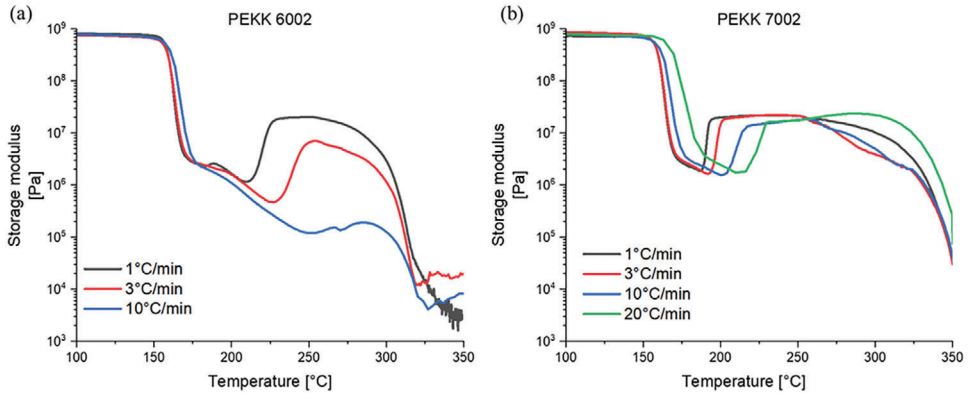

Figure 4. DMTA profiles for a) PEKK 6002 measured with 1, 3 °C min^{-1}, & 10 °C and b) PEKK 7002 measured with 1, 3, 10 °C min^{-1}, and 20 °C.

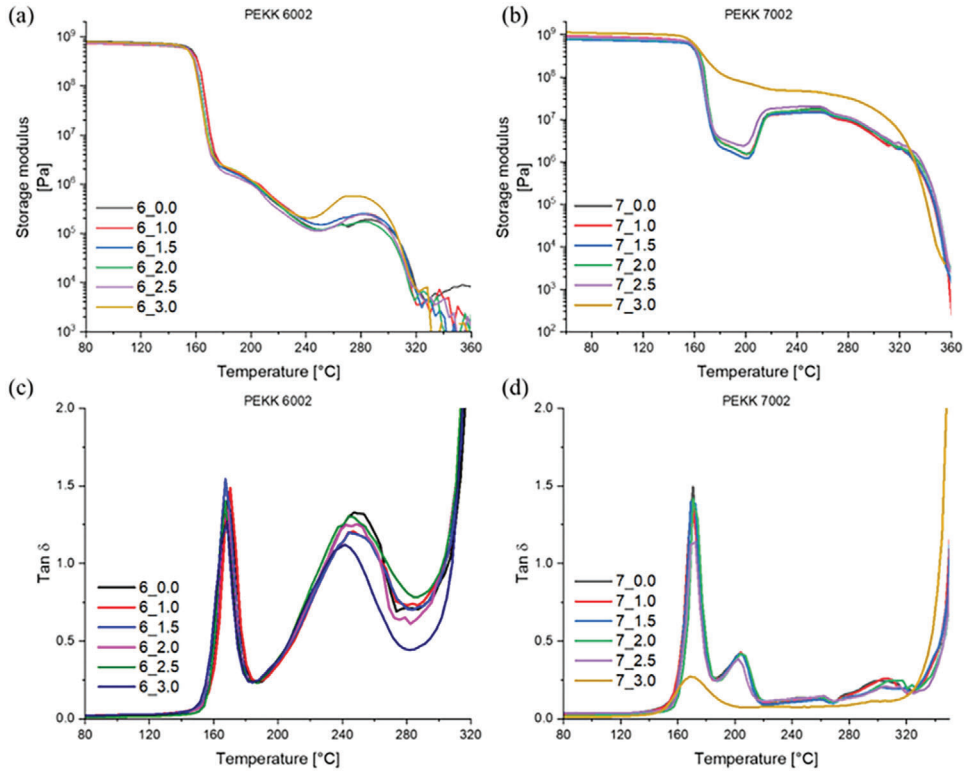

Figure 5. DMTA profiles including storage modulus upper row and tan δ bottom row for PEKK 6002 left-hand side and PEKK 7002 right-hand side. Heating rate 10 °C min^{-1}.

Higher chamber temperature does not increase modulus as it was in the case of the PEEK and PEEK composites.[15,24] Comparable results can be observed for PEKK 7002 for specimens 7_0.0–7_2.5 (which exclude the one obtained at the highest chamber temperature): The storage modulus was 730 MPa (±50), generally similar, independent of the chamber temperature, and nearly identical to the PEKK 6002 samples. The observed high similarity of both sets of samples was due to printing conditions which favored rapid vitrification: below the glass transition temperature, the in situ crystallization process does not take place and the printed body is amorphous (see also amorphous XRD patterns of the corresponding samples in Figure 3).

A different situation is observed for the sample 7_3.0: its storage modulus at 100 °C is significantly higher (namely, 1064 MPa) in comparison to its counterpart 6_3.0 (761 MPa) printed under the same conditions (or with sample 7_2.5: which displays 730 MPa at 100 °C). Crystals formed during the printing process (see corresponding XRD pattern in Figure 3b) are solely responsible for the increase in mechanical properties. The rate of crystallization for 7002 is a bit higher than for 6002 due to a more ordered arrangement of the molecular chain, and as result, this allows for the partial crystallization of PEKK 7002 at the highest tested chamber temperature.

If the post-glass-transition region is considered, the storage modulus at 200 °C is not markedly changed for matrix 6002 printed at different chamber temperatures (but always amorphous—it has a slow crystallization kinetics): it stays in the range between 1.0 and 1.3 MPa. Similar results were obtained for the matrix 7002 printed below glass transition temperature (samples 7_0.0–7_2.5), where crystallization is driven by a slow diffusion process and is not prominent at 200 °C: low modulus in the range of 1.2–2.4 MPa is observed. Only the 7002 specimens printed at the highest temperature around 190 °C are characterized by a markedly increased (by nearly two orders) storage modulus at 200 °C, which reflects the in situ crystallization during the printing process. The achieved storage modulus of 71 MPa is a significant difference in comparison to the other 7002 samples and is caused by printing in a condition that is favorable to the generation of well-defined primary crystalline structure. For the same reason, it also can be noted that the sample 7_3.0 printed at 190 °C does not display any cold crystallization above 200 °C in the DMTA test in Figure 5b: the easily crystallizing fraction of the polymer already is crystallized.

The remaining 7002 specimens, which were all printed below their T_g display a steep increase of the storage modulus at temperatures above 200 °C (see Figure 5b). This is the manifestation of the "cold crystallization" of the amorphous phase and is triggered by the increased segmental mobility of the polymer chains at these higher temperatures. The matrix 7002 has a relativity fast crystallization rate which allows observing an increase in the modulus from around 1.5 MPa (±1) to 15 MPa (±3) as a result of cold crystallization during the DMTA test. For the 6002 specimens, a similar behavior was observed at a bit higher temperature with a less steep step around 250 °C due to the slow rate of crystallization. Also, their storage modulus was increased less significantly if compared to 7002.

The graphs of temperature-dependent loss factor (tan δ) in Figure 5c,d offer a detailed view of the characteristic transition temperatures of the studied materials: PEKK 6002 possesses a glass transition temperature of around 167 °C (a bit lower than PEKK 7002 with T_g at 170 °C) and a melting point of around 310 °C (PEKK 7002: melting point around 340 °C). It can be further observed that the glass transition in both the studied PEKK materials generates a sharp peak (correlating with the steep step in the curve of the temperature-dependent modulus). This indicates very uniform conditions for segmental mobility. The cold crystallization manifests itself by a broader peak, which is overly broad and prominent in case of 6002 and much smaller and narrower in case of 7002. The areas of the mentioned peaks do not correlate with heat absorption or release, but with increasingly plastic character. In the case of cold crystallization peaks, the differences between 6002 and 7002 indicate the difficult crystallization of 6002 versus the relatively smooth crystallization of 7002. The dramatic increase of tan δ above 300 °C corresponds to the melting of the polymer (which means dominant plasticity/viscosity and only very small elasticity). The melting transition is relatively sharp in both materials.

The 3DP specimens printed between 7_0.0 and 7_2.0 show nearly identical characteristics with all the main transition peaks and features overlapping very closely (T_g peak maximum: 170 °C, cold crystallization peak: 205 °C, see Figure 5d). When the sample was printed with a chamber temperature of 144 °C (7_2.5), it is possible to notice a gentle decrease in both tan δ peaks because of immobilization of the polymer chain by a small amount of crystalline phase (which means an increased elastic character). This phase was formed even if the chamber temperature of 144 °C, still was below the T_g. More importantly, it should be noted that the conditions during the printing process are not perfectly isothermal. Deposited material is gradually cooled down after deposition from the nozzle preheated to 360 °C and the high enough chamber temperature leads to reduced rate of cooling and gives time to form crystalline domains (before T drops safely far below T_g). Thus, also a slightly raised storage modulus can be observed in Figure 5b. 3DP at a chamber temperature above T_g, hence in the region where polymer chain mobility is limited only by segmental diffusion (which is rapid in 7002) leads to fast crystallization kinetics and allows for the continuous growth of the crystals during the printing process. That was observed for PEKK 7002 printed at around 190 °C (sample 7_3.0). For this sample, the tan δ peak was significantly reduced which directly indicates crosslinking of the polymer chains by crystalline domains (and hence a higher elasticity which means smaller plasticity and smaller tan δ). The second cold crystallization peak around 205 °C is not present at all in the graph of 7_3.0 in Figure 5d because the crystalline phase already formed in full extent during the printing. Thus, the storage modulus of 7_3.0 was the highest (see Figure 5b) and the thermal operation window is widest for 7_3.0. The PEKK 6002 with slow crystallization rate does not allow to build in situ crystalline phase during printing, which is illustrated by Figure 5a,c.

3.1.4. Morphology

Solidification of the PEKK 6002 after deposition takes more time due to the more amorphous character of the materials with higher content of isophthalic acid. This leads to an increase of surface roughness, especially in comparison to 7002 printed with the current of the lamps was set at 3 A, see **Figure 6** mag. x0.25k. A faster crystallization rate helps to increase the surface finish of the printed part and reduce the stringing. Higher magnification reveals the semicrystalline character of both materials. The slow crystallization rate of 6002 exposes the amorphous character of the matrix with the suppressed formation of the spherulites, visible as globules surrounded by an amorphous matrix. The globules could transform into spherulites if there would be enough energy delivered in form of heat for a longer period. A similar observation was made for CF/PEEK where the formation of the spherulites was partially stopped by the thermo-dissipative character of the CF filler at room temperature.[24] For PEKK 7002 with faster crystallization kinetics, it was possible to observe a larger amount of equally distributed crystallization centers in comparison to the PEKK 6002 (Figure 6 mag. x5k). The crystallization process was also inhibited and characteristic globules or short lamellae with diameter around 30 nm are visible as whiter branches in Figure 6 mag. x10k. Those areas are surrounded—not as it was in the case of PEKK 6002 by an amorphous matrix—but also by a well-defined crystallized matrix that forms a structure of short, interconnected needles with the same 30 nm diameter. A similar observation was made for PEEK and its CF/PEEK

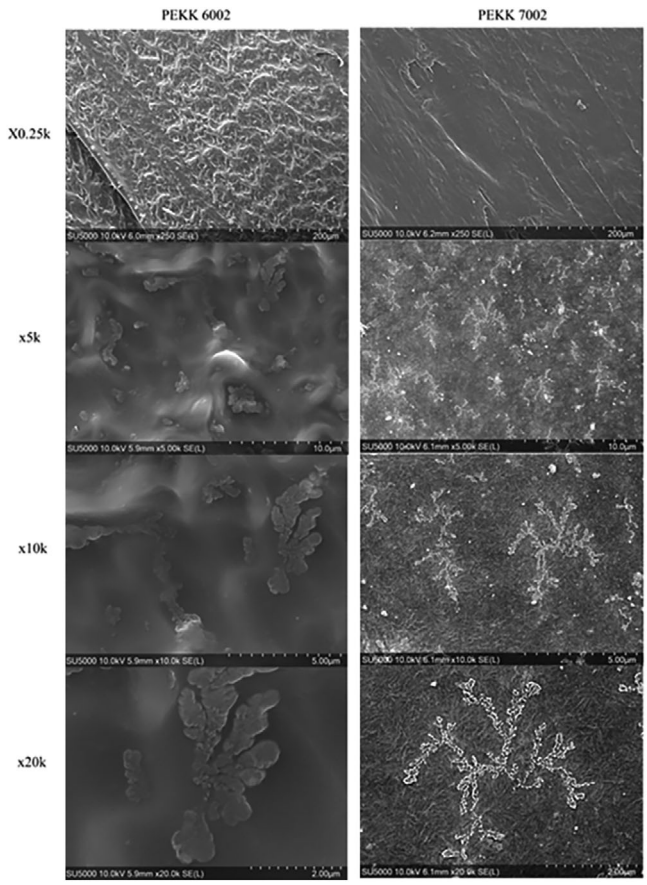

Figure 6. Top layer of the 3DP specimens printed with lamp current 3 A.

composite where the diameter of the lamellae was around 20–30 nm for spherulites.[15,24]

3.2. Printing Condition Effect

Nozzle temperature role: It is possible to observe recent research tends to increase the temperature in the nozzle up to 500 °C, and to print slowly to achieve better mechanical properties. The nozzle then actively participates in heating the already printed layers (see Figure 3a) and the highest temperature at the top few layers is clearly visible.[31] However, this is not a solution for complex structures where retraction of the printing head is required, because of the viscosity of the highly temperature-dependent polymer melt drops and excessive nozzle stringing can be observed in such cases leading to the reduction of the quality of the printed object.

Building plate temperature role: For stabilization on the aluminum sheet without any additional treatment, the temperatures where nucleation controls the process of crystallization are required. Extensive crystallization causes the shrinking of the material due to reduction of the specific volume and more packed chain organization, which leads to object warping. Recommended temperatures are PEEK—280 °C, PEKK 7002—200 °C, and PEKK 6002—180 °C when aluminum plate is used.

Chamber temperature role: It should be adjusted to the material crystallization kinetics and part size to allow deposition of the new layer on a still amorphous part surface, to achieve a good interlayer connection.

3.3. Crystallization Controlled by Temperature and Material Crystallization Kinetics

The crystallization rate is essential for the successful additive manufacturing of semicrystalline polymers and should be taken into consideration during the selection of the materials. When the crystallization rate is too slow as it was in PEKK 6002, it is not possible to print samples rich in the crystalline phase. Theoretically, it would be possible to increase the temperature in the chamber to a level where the crystallization rate is the highest: for PEKK 6002, it is 230 °C. But the temperature 167 °C was already too high from practical point of view: the cooling fan system was not enough efficient, and the polymer had problems with proper solidification after deposition, which led to increased roughness and reduction of accuracy, see Figure 6, x0.25k. A similar phenomenon was observed for PEEK.[32]

The crystalline fraction is responsible for the chemical, thermal, and mechanical properties of the 3D printed object. If the object is printed with a member of the PAEK family of polymers as an amorphous body, its thermal operating window is limited by the glass transition temperature. Chemical resistance is not provided when the crystalline fraction is not present, and mechanical properties such as Young's modulus are close to other amorphous advanced or engineering plastics. When the same material is printed with a high level of primary crystals, the thermal operating window can reach temperatures up to 260 °C. Chemical resistance is improved by the crystalline fraction which does not allow for penetration of small molecules of solvent, base, or acid between the well-ordered and compactly stacked polymer chains. Finally, the Young's modulus of such specimens is significantly higher even in comparison to injection molded specimens.[24]

The above information can suggest that polymers with fast crystallization rates such as PEEK should be the first choice. For some processes such as injection molding, quick crystallization is essential for increasing productivity and thus reducing production costs, but not for AM. Too fast crystallization rate can lead to extensive shrinking and to difficulty in the stabilization of the 3D printed part. The shrinking is due to the rearrangement of molecular chains into a more compact structure. The specific volume is reduced, which leads to shrinking followed by warping. For PEEK, it was necessary to print at 280 °C (chamber temperature) to avoid warping and detachment of the printed part from the building plate during the printing of a wall sample.[33] Whereas PEKK 6002 is stable on platform already at 180 °C and PEKK 7002 can be printed at 200 °C, so this temperature was selected to print both PEKK 6002 and 7002, to keep consistent processing conditions.

The temperature for PEEK printing must be so high to reduce the crystallization rate by slowing down the nucleation process. The fastest crystallization rate for PEEK is around 230 °C. At 280 °C, it is slowed down about ten times.[22] At elevated temperatures close to melting point of the semicrystalline polymer, the

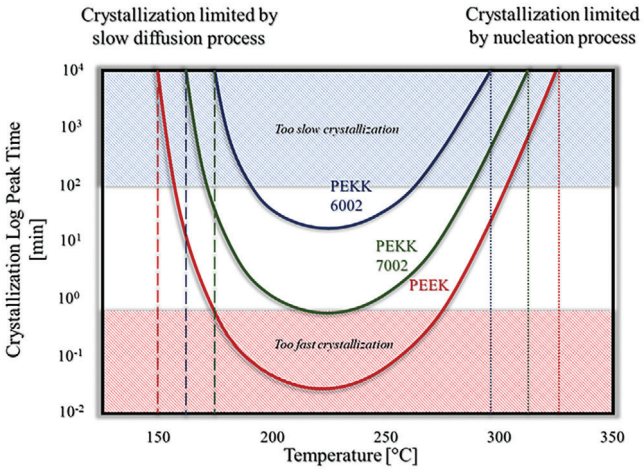

Figure 7. Crystallization kinetics for PEEK, PEKK 6002, and PEKK 7002.[17,18,27,36]

crystallization is controlled by nucleation. Generally, the crystallization can be slowed down by increasing temperature, see **Figure 7**. On the other hand, at low-temperature, crystallization is controlled by the slow process of segmental diffusion (see Figure 7), and this is a second way how it is possible to slow down the crystallization rate of the semicrystalline polymer.[34] However, stabilization of the printed object is not possible to achieve at a low temperature close to the glass transition temperature: the polymers printed below T_g instantly "freeze" due to the significant difference in temperature between the nozzle and the building plate, and the material does not want to stick to the building plate. Especially, it is visible for the PEEK with high melting temperature and relatively low T_g, see Table 1. Material is often printed with nozzle temperatures between 400 and 450 °C. To achieve a relatively slow crystallization rate limited by diffusion, a chamber temperature of 160 °C would be required. In the best scenario, the difference between the surface of the printed object and the deposited fresh material would be 240 °C, which obviously leads to interlayer imperfection such as voids and microcracks.[35] Thus, the material printed is not efficiently connected by chain entanglements (physical crosslinks) and the observed properties in the *Z*-direction are not even close to the performance of an injection molded specimen. For this reason, PEEK printing should be controlled by the nucleation process at elevated temperatures, not by diffusion at low ones.

Controlling temperature which controls crystallization rate is one way to be successful in AM of advanced materials and their composites. This can be simply done by the selection of the proper material with a specific crystallization rate to limit the above-described issues. This is a better approach due to the limitation of the equipment which would require heating up the chamber up to 280 °C for PEEK, which is required theoretically for FFF PEEK to limit the anisotropy of printed part and to avoid weak properties in the *Z*-direction. A similar conclusion was made for SLS where authors suggested that the minimal feeding temperature for PEEK powder should be 250 °C.[37] Slower crystallization of the PEKK 7002 printed at around 190 °C gave the possibility to deposit new material on an amorphous not crystallized object layer, where the macromolecular chains were kept over time at elevated temperatures and only after some delay gradually arranged into crystallites. It is much easier to melt down a semicrystalline polymer in an amorphous state with low thermal stability expressed by T_g than highly thermally stable well-formed primary crystalline domains. The latter, namely, melt at the melting point, which is much higher than T_g. To provide more continuous character of the layers in the *Z*-direction, the moderate crystal formation in PEKK 7002 made it possible to retain the dimensional stability of the part, which was not retained for PEKK 6002 with too slow crystallization kinetics.

It is difficult to print polymer with slow crystallization kinetics and high crystalline fraction in situ. PEKK 6002 is an example of this type of semicrystalline polymer: it is easy to print without excessive warping. The material is characterized by a strong interlayer connection due to the amorphous character of the body. So, a newly deposited layer is welded with amorphous PEKK with thermal stability up to T_g which is around 160 °C. However, for generating the crystalline structure, post-processing would be essential.

The opposite behavior is observed for polymers with fast crystallization kinetics such as PEEK, in which crystallites are formed instantly at temperatures above glass transition temperature. Due to the high tendency for the reorganization of molecular chain, extensive shrinking is observed which leads to warping and poor connection between layers. An elevated level of crystallinity limits the fine interlayer connection. This is because the polymer melt cannot be effectively welded to a surface rich in primary crystallites, which start to melt around 280 °C and where the crystals also work as a thermal shield.

Semicrystalline polymers such as PEKK 7002 with moderate crystallization kinetics allowed the deposition of the new layer in an amorphous state, providing a fine bond, as in the case of a polymer with a slow crystallization rate. The primary and secondary crystallites form slowly during the 3DP process, sometime after the deposition of the respective layer. Thus, it is possible to print both fully amorphous, as well as in situ crystallized parts. This was achieved by tuning the chamber temperature at 132 °C (below T_g) so that the part was printed as amorphous, or at 190 °C (above T_g) where part was rich in crystalline domains. The total content of primary and secondary crystals was 23.4%. Depending on the selected regime, the emerging parts will be characterized by different thermal, chemical, and mechanical properties.

4. Conclusions

Two main strategies for controlling the crystallization process were presented allowing for successfully printing with advanced semicrystalline polymers PEKK 6002, PEKK 7002, PEEK, and their composites. Crystallization kinetics can be controlled in the two areas at low temperatures by slow diffusion and at high temperatures by limiting the nucleation process.

A more suitable method of controlling the crystallization process is a selection of materials with moderate crystallization kinetics, which gives more ability to adjust the mechanical properties of the 3D printed body according to needs. Advanced polymers can be divided into three groups with slow, moderate, and fast crystallization kinetics.

The PEKK 7002 3DP part with high crystallinity content will have a wider thermal operating window up to 260–280 °C till the temperature region where primary crystallites begin to melt. Chemical resistance will be provided to the part along with a higher Young's modulus and stress at break, but lower impact toughness and elongation at break, if compared to "counterpart product" printed as amorphous.

The PEKK family of polymers starts to prevail as a better material for AM. It is easier to extrude filaments from PEKK due to lower melting temperatures combined with higher glass transition temperature, so even printed amorphous bodies possess a bit wider application in comparison to PEEK. The specific condition during the experiment allowed for the first time to print PEKK 7002 with tailored mechanical, thermal, and chemical properties as amorphous or in situ crystallized.

Acknowledgements

The North-West Centre for Advanced Manufacturing (NW CAM) project was supported by the European Union's INTERREG VA Programme, managed by the Special EU Programmes Body (SEUPB). The views and opinions in this document do not necessarily reflect those of the European Commission or the Special EU Programmes Body (SEUPB). For further information about NW CAM, the lead partner, Catalyst, can be contacted for details. A.B. acknowledges the Royal Academy of Engineering for supporting him with the award of an Industrial Fellowship (IF2122\130).

Conflict of Interest

The authors declare no conflict of interest.

Data Availability Statement

The data that support the findings of this study are available on request from the corresponding author. The data are not publicly available due to privacy or ethical restrictions.

Keywords

3D printing, crystallization kinetics, FFF, PEEK, PEKK

Received: December 1, 2022
Revised: February 9, 2023
Published online:

[1] M. Garcia-Leiner, B. Streifel, C. Basgül, D. W. Macdonald, S. M. Kurtz, *Polym. Int.* **2021**, *70*, 1128.
[2] S.-L. Gao, J.-K. Kim, *Composites, Part A* **2000**, *31*, 517.
[3] S. Turri, T. Trombetta, M. Levi, *Macromol. Mater. Eng.* **2000**, *283*, 153.
[4] P. G. Mongan, V. Modi, J. W. Mclaughlin, E. P. Hinchy, R. M. O'higgins, N. P. O'dowd, C. T. Mccarthy, *J. Intell. Manuf.* **2022**, *33*, 1125.
[5] E. Rezvani Ghomi, S. K. Eshkalak, S. Singh, A. Chinnappan, S. Ramakrishna, R. Narayan, *Rapid Prototyping J.* **2021**, *27*, 592.
[6] S. Tas, B. Zoetebier, O. S. Sukas, M. Bayraktar, M. Hempenius, G. J. Vancso, K. Nijmeijer, *Macromol. Mater. Eng.* **2017**, *302*, 1600381.
[7] L. Pigliaru, L. Paleari, M. Bragaglia, F. Nanni, T. Ghidini, M. Rinaldi, *Synth. Met.* **2021**, *279*, 116857.
[8] P. Tadini, N. Grange, K. Chetehouna, N. Gascoin, S. Senave, I. Reynaud, *Aerosp. Sci. Technol.* **2017**, *65*, 106.
[9] H. Alqurashi, Z. Khurshid, A. U. L. Y. Syed, S. Rashid Habib, D. Rokaya, M. S. Zafar, *J. Adv. Res.* **2021**, *28*, 87.
[10] M. F. Arif, S. Kumar, K. M. Varadarajan, W. J. Cantwell, *Mater. Des.* **2018**, *146*, 249.
[11] S. Fish, J. C. Booth, S. T. Kubiak, W. W. Wroe, A. D. Bryant, D. R. Moser, J. J. Beaman, *Addit. Manuf.* **2015**, *5*, 60.
[12] K. Winter, J. Wilfert, B. Häupler, J. Erlmann, V. Altstädt, *Macromol. Mater. Eng.* **2021**, *307*, 2100528.
[13] C. Shuai, C. Shuai, P. Wu, F. Yuan, P. Feng, Y. Yang, W. Guo, X. Fan, T. Su, S. Peng, C. Gao, *Materials* **2016**, *9*, 934.
[14] P. Peyre, Y. Rouchausse, D. Defauchy, G. Régnier, *J. Mater. Process. Technol.* **2015**, *225*, 326.
[15] K. Rodzen, P. K. Sharma, A. Mcilhagger, M. Mokhtari, F. Dave, D. Tormey, R. Sherlock, B. J. Meenan, A. Boyd, *Polymers* **2021**, *13*, 545.
[16] T. Choupin, B. Fayolle, G. Régnier, C. Paris, J. Cinquin, B. Brulé, *Polymer* **2018**, *155*, 109.
[17] A. M. Gohn, J. Seo, R. H. Colby, R. P. Schaake, R. Androsch, A. M. Rhoades, *Polymer* **2020**, *199*, 122548.
[18] J. Seo, A. M. Gohn, O. Dubin, H. Takahashi, H. Hasegawa, R. Sato, A. M. Rhoades, R. P. Schaake, R. H. Colby, *Polym. Cryst.* **2019**, *2*, 10055.
[19] D. Kemmish, in *Update on the Technology and Applications of Polyaryletherketones*, Smithers Rapra Publishing, Shawbury, UK **2010**, p. 34.
[20] A. Fortney, E. Fossum, *Polymer* **2012**, *53*, 2327.
[21] N. Yi, R. Davies, A. Chaplin, P. Mccutchion, O. Ghita, *Addit. Manuf.* **2021**, *39*, 101843.
[22] H. Pérez-Martín, P. Mackenzie, A. Baidak, C. M. Ó Brádaigh, D. Ray, *Composites, Part B* **2021**, *223*, 109127.
[23] K. Banerjee, M. Debroy, V. K. Balla, S. Bodhak, *J. Mater. Res.* **2021**, *36*, 3877.
[24] K. Rodzen, E. Harkin-Jones, M. Wegrzyn, P. K. Sharma, A. Zhigunov, *Composites, Part A* **2021**, *149*, 106532.
[25] C. Bas, *Eur. Polym. J.* **1995**, *31*, 911.
[26] T. Choupin, B. Fayolle, G. Régnier, C. Paris, J. Cinquin, B. Brulé, *Polymer* **2017**, *111*, 73.
[27] R. M. Ho, S. Z. D. Cheng, B. S. Hsiao, K. H. Gardner, *Macromolecules* **1994**, *27*, 2136.
[28] K. H. Gardner, B. S. Hsiao, R. R. Matheson, B. A. Wood, *Polymer* **1992**, *33*, 2483.
[29] K. H. Gardner, B. S. Hsiao, K. L. Faron, *Polymer* **1994**, *35*, 2290.
[30] A. M. Jonas, T. P. Russell, D. Y. Yoon, *Macromolecules* **1995**, *28*, 8491.
[31] C. A. Chatham, C. E. Zawaski, D. C. Bobbitt, R. B. Moore, T. E. Long, C. B. Williams, *Macromol. Mater. Eng.* **2019**, *304*, 1800764.
[32] I. Baek, O. Kwon, C.-M. Lim, K. Y. Park, C.-J. Bae, *Materials* **2022**, *15*, 898.
[33] K. Rodzen, M. J. Mcivor, P. K. Sharma, J. G. Acheson, A. Mcilhagger, M. Mokhtari, A. Mcferran, J. Ward, B. J. Meenan, A. R. Boyd, *Polymers* **2021**, *13*, 3117.
[34] S. Tan, A. Su, J. Luo, E. Zhou, *Polymer* **1999**, *40*, 1223.
[35] M. Rinaldi, T. Ghidini, F. Cecchini, A. Brandao, F. Nanni, *Composites, Part B* **2018**, *145*, 162.
[36] X. Tardif, B. Pignon, N. Boyard, J. W. P. Schmelzer, V. Sobotka, D. Delaunay, C. Schick, *Polym. Test.* **2014**, *36*, 10.
[37] P. Chen, H. Cai, Z. Li, M. Li, H. Wu, J. Su, S. Wen, Y. Zhou, J. Liu, C. Wang, C. Yan, Y. Shi, *Addit. Manuf.* **2020**, *36*, 101615.

